

Effect of Direct Current Electrowetting on Dielectric on Droplet Impingement Dynamics



K. Niju Mohammed, A. Shebin, E. Mohammed Haseeb, P. S. Tide, Franklin R. John, Ranjith S. Kumar, and S. S. Sreejakumari

Nomenclature

θ	Final contact angle ($^{\circ}$)
θ_0	Initial contact angle ($^{\circ}$)
ε_r	Relative permittivity
ε_0	Permittivity of vacuum (F/m)
d	Dielectric thickness (μm)
γ_{LV}	Surface tension (N/m)
V	Voltage (V)
We	Weber number
v	Characteristic velocity (m/s)

1 Introduction

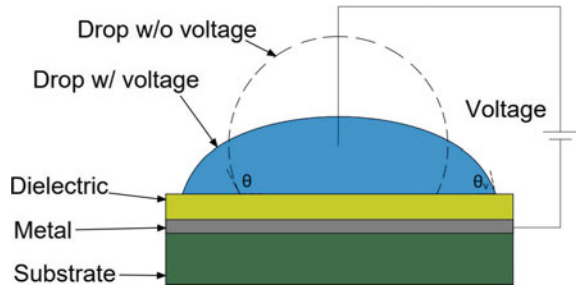
For a few decades, a considerable growth has been witnessed in the field of microfluidics relating to engineering and medical applications [1]. Surface force is more dominant than pressure and body forces at microscale level due to the greater surface area

K. Niju Mohammed · P. S. Tide · F. R. John
Department of Mechanical Engineering, School of Engineering, Cochin University of Science and Technology, Cochin, Kerala, India

K. Niju Mohammed · A. Shebin (✉) · E. Mohammed Haseeb · R. S. Kumar
Micro/Nanofluidics Research Laboratory, College of Engineering, Trivandrum, Kerala 695016, India
e-mail: Shebin.albu@gmail.com

S. S. Sreejakumari
Materials Science and Technology Division, CSIR NIIST, Thiruvananthapuram, Kerala 695019, India

Fig. 1 Schematic of electrowetting on dielectric



to volume ratio [2]. As a result, the manipulation of liquid droplets on the microscale is a tedious task. On the microscale, droplets can be conveniently controlled by creating gradients of parameters like chemical affinity, thermo-capillarity, sound wave, etc. But due to low cost, fine controllability, high rate of switching, and precision, electrostatic actuation draws attention. Electrowetting and dielectric are the two main mechanisms involved in electrostatic actuation [3, 4].

Electrowetting is a physical phenomenon of changing droplet shape by the application of voltage between droplet and surface it is placed. This phenomenon is obvious when we employ electrode surfaces covered with dielectric substances. Figure 1 depicts a typical arrangement of EWOD. The multi-electrode system is also used for manipulating droplet motion [5]. The contact angle decreases when a voltage is applied.

In recent years, the concept of digital microfluidics (DMF) [6] has attracted many researchers in various fields. In DMF, discrete droplets are used instead of continuous flow. It is being employed in a wide spectrum of applications in many scientific domains, from engineering to the biological sciences, including variable focus lenses [7], display technologies [8], fiber optics [9], and lab-on-a-chip applications [10]. EWOD can be used as a platform for performing basic operations of DMF such as generating, splitting, merging, and transporting droplets [11]. Among many other applications, EWOD can be used in hot spot cooling for more efficient and target-specific thermal management of electronics [12].

In this study, experimental analysis of droplet impingement on the EWOD surface has been carried out. Here, a droplet is allowed to free fall onto a hydrophobic surface and analyze the interaction between the surfaces. The water contact angle (WCA) of the substrate (145°) is measured by using a goniometer. The hydrophobic test specimen is prepared using a spray coater and a droplet impingement experiment is done. We conducted a parametric study by varying the droplet diameter, droplet impingement height, and applied voltage.

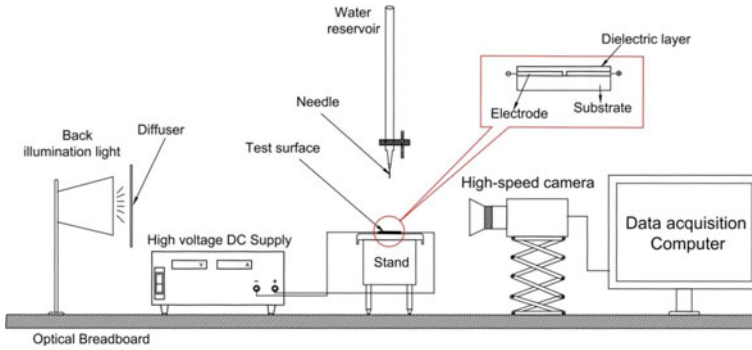


Fig. 2 Illustrative representation of experimental setup

2 Methodology

Figure 2 provides an illustrative representation of the experimental setup. The deionized (DI) water droplets were generated from the water reservoir attached with a flat-headed needle. By regulating the valve on the reservoir, the droplet is formed on the tip of the needle. When the gravitational force exceeds the adhesive and cohesive forces, the droplet fell from the needle.

The EWOD chip ($1'' \times 3''$) is composed of a copper-clad substrate with a gap of $1/64$ inch (0.396 mm) at the middle. On this, a PDMS-Silica nanocomposite was spray-coated using a 1 mm diameter nozzle [13, 14]. It acts as both hydrophobic as well as dielectric coating. The spray-coated substrate was kept at room temperature for curing for at least 24 h.

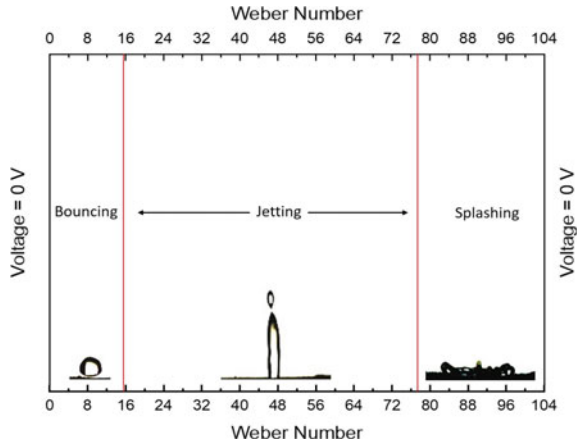
To record the droplet impingement, a high-speed camera was employed at a frame rate of 4500 frames per second. The camera was regulated by the Hi-Spec Camera software, to save the images of the droplet impingement process.

A high-voltage DC source is used to give the required electric signal. The temperature for the experimental condition is set to 26 °C. The terminals of the high-voltage DC source were associated to electrodes by a wire. Initially, the droplet impingement without applying direct current to the EWOD chip was recorded as the reference case. In order to study the droplet impact phenomena, various DC voltages were subsequently applied to the chip. To verify the accuracy and repeatability of the experimental data, each experiment was carried out thrice for each DC voltage.

3 Results and Discussion

A reference droplet impingement experiment was conducted at 0 V to understand the droplet behavior at different Weber numbers. The Weber number indicates the ratio of the inertial force to the surface tension force. The Weber number $We = \rho v^2 D_0 / \sigma$,

Fig. 3 Regimes of droplet impingement on EWOD at 0 V



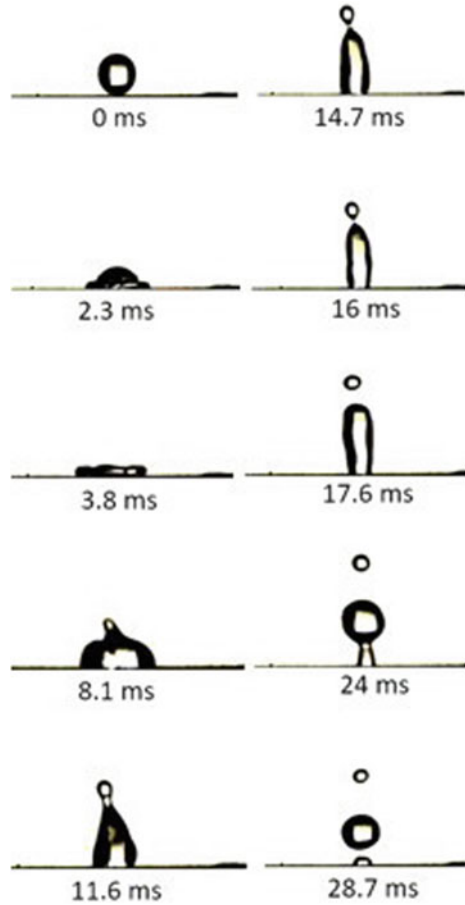
where ρ is the fluid density (kg/m^3) and v is the characteristic velocity (m/s), D_0 is the diameter of droplet (m), and σ is the surface tension of the fluid (N/m). Figure 3 displays bouncing phenomena from $We = 0$ to $We = 15.48$, jetting till $We = 77.4$, and the remaining is splashing. The droplet diameter was 2.76 mm and the contact angle of the PDMS-Silica nanocomposite coat is 145° .

From this reference experimental data, we selected $We = 20.02$ for the study. The impingement velocity was 0.73 m/s. The jetting phenomenon occurred during the droplet impingement on the virgin hydrophobic substrate.

3.1 Dynamics of Droplet Impingement on EWOD Chip Without Voltage

The spreading and retraction of the impingement of the droplet were noted with the aid of the high-speed camera as shown in Fig. 4. Just before collision, the droplet maintained an almost spherical shape. When impinged on the substrate, initially the droplet spreads out due to the inertial force. During this period, the droplet area gradually increases to reach maximum value at 3.8 ms, mimicking a “round pudding” shape. When the surface tension force exceeds the inertial force, the retraction stage begins. Here spreading diameter of the droplet is reduced gradually and attained its peak height at 14.7 ms. During retraction, necking is observed. As shown in Fig. 4, jetting occurred at 16 ms. Necking results from a conflict between a capillary retraction that takes place when the bulbous end increases, owing to surface tension and a pressure-driven flow from the jet that feeds the size of the top droplet. As the jet is stretched thinner due to inertial forces in the axial direction, the neck thins and eventually ruptures which ejects the satellite droplet upward due to the abrupt disconnection from the main body of the jet [15]. As shown in Fig. 4, the small droplet stayed in the air and the large droplets clung to the surface, yielding an elongation.

Fig. 4 Droplet impingement process at $We = 20.02$ on EWOD chip without voltage



During jetting, the small droplet stays in the air and the large droplet gets adhered to the substrate leading to elongation at 17.6 ms. It again breaks into large and small droplets. Here small droplets adhere to the surface. The large droplet hung on the air until its energy is being consumed, and then rests on the hydrophobic substrate. This is in line with the findings reported in [16–19].

3.2 Dynamics of Droplet Impingement on EWOD Chips with Voltage

When DC voltages are applied on the EWOD chip, the droplet impingement same as that of the reference case (0 V, $We = 20.02$) was recorded and is shown in Fig. 5. For a DC voltage of 250 V applied on EWOD, from 0 to 3.8 ms, the initial droplet

spreading dynamics upon impact as shown in Fig. 5 was similar compared with the scenario without voltages shown in Fig. 4. When the maximum area is reached by the droplet, the spreading diameter of the droplet upon voltage application was larger than that in the no voltage case. The spreading droplet shape was not as smooth and flat compared with the reference case due to the electrostatic force produced by the EWOD. At 3.9 ms to 4.1 ms, the droplet made varying contact angles with the left and right sides. This contact angle variation is induced by a Laplacian pressure difference generated in the droplet which resulted in the radial shift of the droplet to occur. At 15 ms time frame, the droplet entirely shifted to the right electrode resulting in breaking off the electric circuit in the EWOD chip. Eventually, the droplet was not regulated by EWOD anymore and the droplet gets stabilized at 31 ms.

In the retraction phase, the droplet dynamics and shape were distinct from the no voltage case depicted in Fig. 5. The water droplet does not separate from EWOD test specimen during the retraction process until it completely shifts to one electrode. During the entire retraction phase, the droplet is adhered to the EWOD chip without jetting and it then gets stabilized.

Fig. 5 Droplet impingement process at $We = 20.02$ on EWOD chip with a DC voltage of 250 V

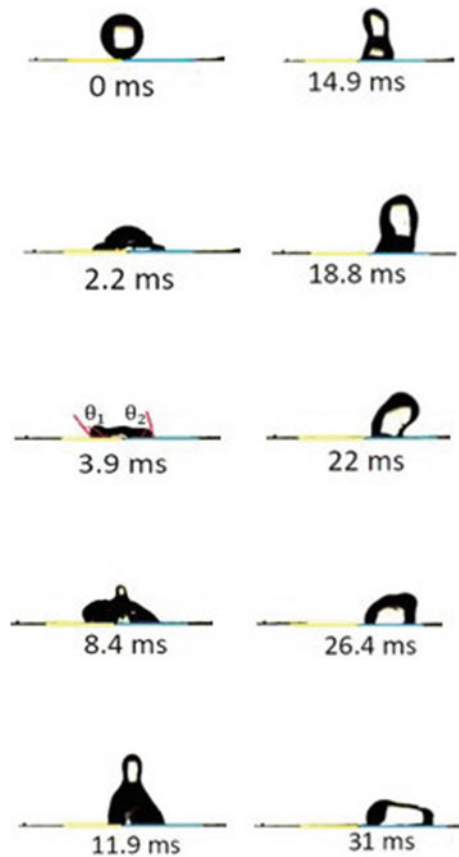
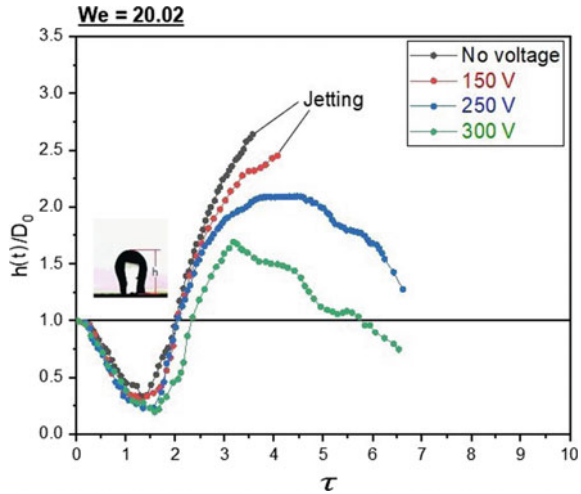


Fig. 6 Variation in droplet height with voltage over time

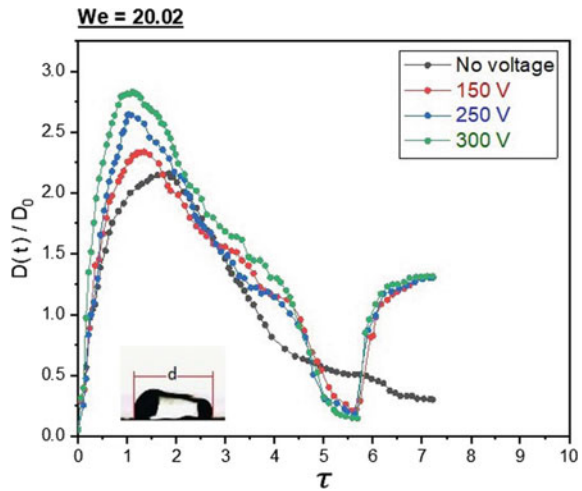


3.3 Effect of Voltage on Droplet Height and Diameter on Droplet Impact Dynamics.

The inhibition of jetting of the droplet took place by the application of DC voltage to the EWOD as seen in Fig. 5. To understand the effect of voltage on droplet dynamics, the droplet impingement trials were performed at different voltages. The height and diameter of the impacting droplet are the two important parameters for detailing the energy conversion during the impingement process. The kinetic energy was transformed into surface energy and the droplet spreads radially. Figure 6 shows the variation of the height of the droplet at various voltages. The height is defined in this case as the vertical length of the droplet from the EWOD chip to the top of the droplet. At 0 ms, the droplet touched the EWOD chip and its height was nearly the diameter of the droplet (2.76 mm).

As shown in Fig. 4, at no voltage condition, the impingement of the droplet undertakes spreading, and the maximum spreading diameter (5.98 mm) was obtained between 3.5 and 4.3 ms. At the same time, it reaches a minimum height (0.928 mm) from the surface. These conditions hold good for a duration of 2.3 ms. In this phase, the droplet velocity is reduced to zero and it attains maximum spreading by converting the kinetic energy of droplet into its surface energy. The minimum height was 0.928 mm and the maximum droplet diameter without voltage was 5.98 mm as given in the Figs. 6 and 7, respectively. Here τ is the nondimensionalized resident time and expressed as $\tau = \frac{t}{D_0/V_{im}}$ [20], where V_{im} is the droplet impact velocity. The maximum spreading phase of the droplet was followed by retraction and jetting, as a result of which the droplet diameter continued to reduce and reaches a minimum and the height becomes maximum. On application of DC voltage to the EWOD, the spreading diameter and height of the droplet shows distinct behavior from the droplet impact without voltage, i.e., the maximum droplet diameter is increased, and

Fig. 7 Variation in diameter of the droplet with voltage over time



the maximum height gets decreased, e.g., Fig. 7 shows that applying a DC voltage of 300 V results in a maximum droplet diameter of 7.78 mm, which is 30% larger compared with that of the impinging droplet diameter without the application of voltage (5.98 mm), and in the case of height also shows significant changes.

A new difference arises in the retraction phase. The diameter of the droplet impinging the DC-EWOD showed some peaks and troughs when the droplet contacted the surface of EWOD, a change in the contact angle occurred following the Young–Lippmann equation.

$$\cos \theta = \cos \theta_0 + \frac{\epsilon_0 \epsilon_r}{2\gamma_{LV}d} V^2 \tag{1}$$

where θ_0 is the initial contact angle, θ is the final contact angle, ϵ_r is the relative permittivity, ϵ_0 is the permittivity of vacuum, d is the dielectric thickness, and γ_{LV} is the surface tension between liquid and air.

When different values of DC voltages were applied, the contact angle of the droplet decreased according to Eq. (1). Table 1 gives the variation of contact angle with voltages.

Table 1 Variation of contact angle with voltages

Voltage (V)	Theoretical contact angle (°)	Nature of surface
0	145	Nearly superhydrophobic
150	117	Hydrophobic
200	100	Hydrophobic
250	79	Hydrophilic
300	50	Hydrophilic

When the DC voltage was zero, the contact angle of the impinging droplet was not affected by EWOD. When the DC voltage was applied to the EWOD chip, induced a fluctuation in the diameter of the impinging droplet. As a result, its retraction phase could not proceed normally, causing the droplet to adhere to the hydrophilic surface created due to electrostatic forces and as explained by the Young-Lipmann equation. As the voltage is decreased from 300 to 150 V, the droplet diameter continued to reduce because of the decrease in the intensity of voltage as shown in Fig. 9. This reduction in voltage also changes the contact angle of the impinging droplet. On further reducing the voltages to a low value like 50 V, the diameter of the impinging droplet was similar to the case without voltage. As the DC signal was continuously applied on the EWOD chip, in 3.9 ms, the droplet made a different contact angle on the right and left sides and this varying contact angle resulted in a Laplacian pressure difference across the droplet which resulted in motion in radial direction. At 15 ms, the droplet completely covered the right electrode, and the electric circuit in the EWOD configuration was cut off. As a result, the droplet was not controlled by EWOD and gets stabilized after a partial rebound nearly at 31 ms. Figure 8 shows the variation in the maximum height of the droplet in accordance with different voltages. h_{max} is the maximum vertical distance from the EWOD chip to the top of the droplet. At low voltage, jetting is observed. As the applied voltage increases h_{max} decreases and jetting gets inhibited. Figure 9 shows the maximum diameter of droplet spread the droplet. d_{max} increases due to an increase in hydrophilic nature imparted by a rise in voltage.

Fig. 8 Variation of h_{max} with voltage

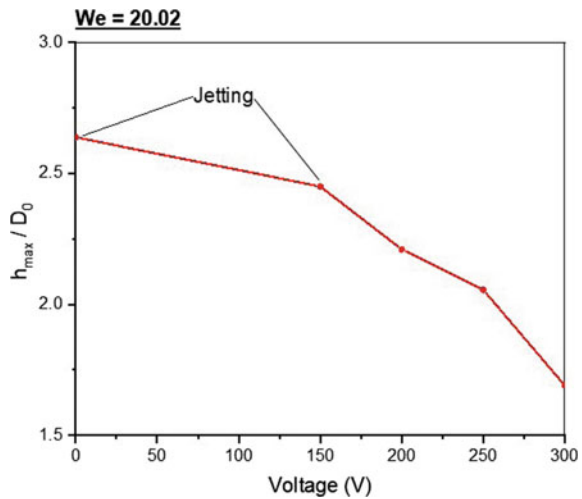
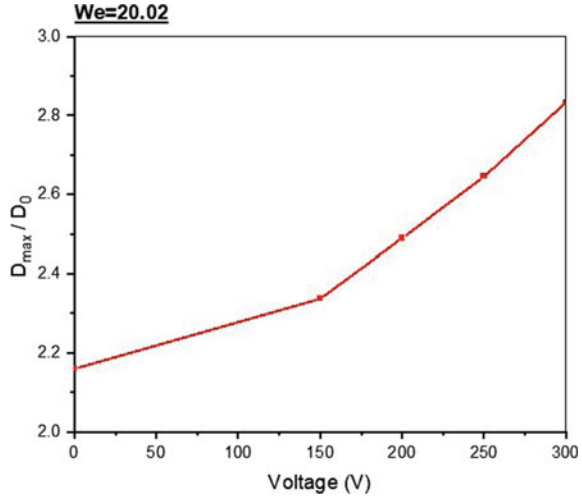


Fig. 9 Variation of d_{\max} with voltage



4 Conclusions

In this study, direct current electrowetting on dielectric (DC-EWOD) regulates the motion of a droplet impinging on a hydrophobic substrate. At weber number of 20.02, jetting is inhibited by the application of direct current to the EWOD and the droplet got shifted to one side. On applying the DC voltage on the EWOD chip, the diameter of droplet spreading got increased and the droplet height got decreased during the spreading and retraction processes, respectively. The results showed that the magnitude of the voltage had a dominating effect on jetting inhibition. The results help to provide a reference for future research on applications, including electronic cooling, inkjet printing, and lab-on-chip applications.

Acknowledgements The authors would like to acknowledge CSIR-NIIST Pappanamcode for helping with the fabrication of the EWOD chip.

References

1. Lim B, Vavassori P, Sooryakumar R, Kim C (2016) Nano/micro-scale magnetophoretic devices for biomedical applications. *J Phys D Appl Phys* 50:033002
2. Datta S, Das AK, Das PK (2017) Influence of surface contact angle on uphill motion of droplets due to electrostatic actuation. In: *Fluid mechanics and fluid power—contemporary research*. Springer, pp 1305–1313
3. Datta S, Kumar P, Das AK (2019) Manipulation of droplets by electrostatic actuation and the related hydrodynamics. *J Indian Inst Sci* 99(1):121–141
4. Lee J, Moon H, Fowler J, Schoellhammer T, Kim C-J (2002) Electrowetting and electrowetting-on-dielectric for microscale liquid handling. *Sensors Actuators, A* 95(2):259–268. Papers from the Proceedings of the 14th IEEE International conference on microelectromechanical systems

5. Accardo A, Mecarini F, Leoncini M, Brandi F, Di Cola E, Burghammer M, Riekkel C, Di Fabrizio E (2013) Fast, active droplet interaction: coalescence and reactive mixing controlled by electrowetting on a superhydrophobic surface. *Lab Chip* 13:332–335
6. Choi K, Ng AH, Fobel R, Wheeler AR (2012) Digital microfluidics. *Annu Rev Anal Chem* 5:413–440
7. Doering C, Strassner J, Fouckhardt H (2021) Microdroplet actuation via light line optoelectrowetting (ll-ow). *Int J Anal Chem* 2021
8. Li J et al (2020) Current commercialization status of electrowetting-on-dielectric (ewod) digital microfluidics. *Lab Chip* 20(10):1705–1712
9. Vo PQ, Husser MC, Ahmadi F, Sinha H, Shih SC (2017) Image-based feedback and analysis system for digital microfluidics. *Lab Chip* 17(20):3437–3446
10. Fair RB (2007) Digital microfluidics: is a true lab-on-a-chip possible? *Microfluid Nanofluid* 3(3):245–281
11. Geng H, Feng J, Stabryla LM, Cho SK (2017) Dielectrowetting manipulation for digital microfluidics: creating, transporting, splitting, and merging of droplets. *Lab Chip* 17(6):1060–1068
12. Bindiganavale G, You SM, Moon H (2014) Study of hotspot cooling using electrowetting on dielectric digital microfluidic system. In: 2014 IEEE 27th International conference on micro electro mechanical systems (MEMS). IEEE, pp 1039–1042
13. Bharathidasan T, Narayanan TN, Sathyanaryanan S, Sreejakumari S (2015) Above 170° water contact angle and oleophobicity of fluorinated graphene oxide based transparent polymeric films. *Carbon* 84:207–213
14. Basu BJ, Bharathidasan T, Anandan C (2013) Superhydrophobic oleophobic PDMS-silica nanocomposite coating. *Surf Innov* 1(1):40–51
15. Asai B (2022) Outcomes following droplet impact on a hydrophilic substrate: spreading, jetting, and partial rebound. PhD Thesis, Washington State University
16. Tan J, Wang H, Sun M, Tian P, Wang Y, Wang K, Jiang D (2021) Regulating droplet impact on a solid hydrophobic surface through alternating current electrowetting-on-dielectric. *Phys Fluids* 33(4):042101
17. Nandakumar Chandran K, Naveen P, Abhilash R, Kumar Ranjith S (2021) Theoretical modelling of droplet extension on hydrophobic surfaces. *Int J Comput Fluid Dyn* 35(7):534–548
18. Rajesh RS, Naveen P, Krishnakumar K, Ranjith SK (2019) Dynamics of single droplet impact on cylindrically-curved super-heated surfaces. *Exp Thermal Fluid Sci* 101:251–262
19. Ulahannan L, Krishnakumar K, Nair AR, Ranjith SK (2021) An experimental study on the effect of nanoparticle shape on the dynamics of Leidenfrost droplet impingement. *Exp Comput Multiphase Flow* 3(1):47–58
20. Chen R-H, Chiu S-L, Lin T-H (2007) Resident time of a compound drop impinging on a hot surface. *Appl Therm Eng* 27(11–12):2079–2085